EXTENDED PDF FORMAT
SPONSORED BY

Salt Tolerance Conferred by Overexpression of a Vacuolar Na +/H+ Antiport in Arabidopsis

Maris P. Apse, *et al.*

Science **285**, 1256 (1999);
DOI: 10.1126/science.285.5431.1256

The following resources related to this article are available online at www.sciencemag.org (this information is current as of April 28, 2009):

Updated information and services, including high-resolution figures, can be found in the online version of this article at:
http://www.sciencemag.org/cgi/content/full/285/5431/1256

This article **cites 12 articles**, 7 of which can be accessed for free:
http://www.sciencemag.org/cgi/content/full/285/5431/1256#otherarticles

This article has been **cited by** 415 article(s) on the ISI Web of Science.

This article has been **cited by** 92 articles hosted by HighWire Press; see:
http://www.sciencemag.org/cgi/content/full/285/5431/1256#otherarticles

This article appears in the following **subject collections**:
Botany
http://www.sciencemag.org/cgi/collection/botany

Information about obtaining **reprints** of this article or about obtaining **permission to reproduce this article** in whole or in part can be found at:
http://www.sciencemag.org/about/permissions.dtl

Downloaded from www.sciencemag.org on April 28, 2009

Science (print ISSN 0036-8075; online ISSN 1095-9203) is published weekly, except the last week in December, by the American Association for the Advancement of Science, 1200 New York Avenue NW, Washington, DC 20005. Copyright 1999 by the American Association for the Advancement of Science; all rights reserved. The title *Science* is a registered trademark of AAAS.

observed initial velocity (~3 μm/min) of the front. Thus, the gradient of chemical potential rather than the thickness gradient is responsible for initiating the growing dewetting front. Once the dewetting front advances, one would expect the driving force exerted by the Marangoni flow to decay. The front, however, continues to move, driven by the reduction in free energy associated with progressive exposure of the lower layer.

In Fig. 5B, we schematically show a possible mechanism, suggested by the above results, connecting the motion of the liquid rim with the accelerated hole rupture ahead of it. A liquid drop or a rim resting on a liquid substrate will deform the contact area between the two fluids. As the rim begins to move, its flow distorts the lower film and leads to a wave of the substrate liquid forming ahead of the moving droplet. Similarly, a droplet spreading on top of another liquid leads to the formation of a wave ahead of the spreading precursor film. The wave locally thins the upper layer to a thickness $h < h_0$, the unperturbed thickness, to form a zone of higher rupture probability (recalling that, for a spinodal dewetting process, $\tau \sim h^5$). This mechanism results in a line of "preferred breakup points" ahead of the dewetting front and qualitatively explains both the directed growth and the variation of hole diameters shown in Fig. 3. For the case of liquid mixtures, this process represents an alternative and more rapid pathway to the classical processes associated with spinodal dewetting or with heterogeneous nucleation mechanisms.

References and Notes

1. P. Weiss, *Sci. News* **155**, 28 (1999).
2. K. Binder, *Rep. Prog. Phys.* **50**, 783 (1987).
3. L. Leger and J. F. Joanny, *ibid.* **55**, 431 (1992).
4. F. Brochard-Wyart, J. M. diMeglio, D. Quéré, P. G. deGennes, *Langmuir* **7**, 335 (1991); F. Brochard-Wyart and J. Daillant, *Can. J. Phys.* **68**, 1084 (1990).
5. See, for example, S. Herminghaus *et al.*, *Science* **282**, 916 (1998); G. Reiter, *Langmuir* **9**, 1344 (1993); T. G. Stange, D. F. Evans, W. A. Hendrickson, *ibid.* **13**, 4459 (1997); J. Bischof, D. Scherer, S. Herminghaus, P. Leiderer, *Phys. Rev. Lett.* **77**, 1536 (1996); K. Jacobs, S. Herminghaus, K. Mecke, *Langmuir* **14**, 965 (1998).
6. R. Xie, A. Karim, J. F. Douglas, C. C. Han, R. A. Weiss, *Phys. Rev. Lett.* **81**, 1251 (1998).
7. F. Brochard-Wyart, P. Martin, C. Redon, *Langmuir* **9**, 3682 (1993).
8. We observed a qualitatively similar phenomenon with the nondeuterated oligomers OS-OEP. In that system, the OEP-rich phase aligns at the air interface, and the OS-rich phase aligns at the gold surface.
9. White-light interference microscopy (NewView 200, Zygo, Middlefield, CT) was used for profiling the detailed shape of a liquid droplet on top of the liquid film. In this three-dimensional technique, an image of the surface is obtained by analyzing the interference pattern formed by a reference and a sample beam. The technique provides a detailed profile of the contact line with subnanometric resolution in the vertical direction and micrometer resolution in the lateral direction.
10. T. Kerle *et al.*, *Acta Polym.* **48**, 548 (1997).
11. U. K. Chaturvedi *et al.*, *Appl. Phys. Lett.* **56**, 1228 (1990).
12. F. Scheffold *et al.*, *J. Chem. Phys.* **104**, 8786 (1996).
13. K. Binder, *ibid.* **79**, 6387 (1983).
14. F. Brochard-Wyart, G. Debregeas, P. G. deGennes, *Colloid Polym. Sci.* **274**, 70 (1996).
15. J. F. Joanny, *Physicochem. Hydrodyn.* **9**, 183 (1987).
16. H. Linde *et al.*, *J. Colloid Interface Sci.* **188**, 16 (1997).
17. X. Fanton and A. M. Cazabat, *Langmuir* **14**, 2554 (1998).
18. With $h = 200 \times 10^{-9}$ m, $\eta = 50$ P, $\delta\gamma = 2 \times 10^{-3}$ N/m, and $\delta x = 1$ mm, shear velocity $v_x = 6$ μm/min.

19. We are grateful to L. J. Fetters and M. Wilhelm for kindly donating the OEP and dOS oligomers. We thank J. F. Joanny, S. Safran, and H. Grüll for enlightening discussions and the U.S.–Israel Binational Science Foundation (grant 95-147), the Wolfson Family Charitable Trust (to R.Y.-R.), the German-Israel Foundation (grant I-568-275.0597), and the Israel Ministry of Science (Tashtiot Program) for support.

12 April 1999; accepted 9 July 1999

Salt Tolerance Conferred by Overexpression of a Vacuolar Na^+/H^+ Antiport in *Arabidopsis*

Maris P. Apse,* Gilad S. Aharon,* Wayne A. Snedden, Eduardo Blumwald†

Agricultural productivity is severely affected by soil salinity. One possible mechanism by which plants could survive salt stress is to compartmentalize sodium ions away from the cytosol. Overexpression of a vacuolar Na^+/H^+ antiport from *Arabidopsis thaliana* in *Arabidopsis* plants promotes sustained growth and development in soil watered with up to 200 millimolar sodium chloride. This salinity tolerance was correlated with higher-than-normal levels of *AtNHX1* transcripts, protein, and vacuolar Na^+/H^+ (sodium/proton) antiport activity. These results demonstrate the feasibility of engineering salt tolerance in plants.

Salinity stress is one of the most serious factors limiting the productivity of agricultural crops. The detrimental effects of salt on plants are a consequence of both a water deficit resulting in osmotic stress and the effects of excess sodium ions on critical biochemical processes (*1*). In order to tolerate high levels of salt, plants should be able to utilize ions for osmotic adjustment and internally distribute these ions to keep sodium away from the sites of metabolism (*1*). Plant cells are structurally well suited for the sequestration of ions because of the presence of large, membrane-bound vacuoles. It has been proposed that in salt-tolerant plants, the compartmentation of Na^+ into vacuoles, through the operation of a vacuolar Na^+/H^+ antiport, provides an efficient mechanism to avert the deleterious effects of Na^+ in the cytosol and maintains osmotic balance by using Na^+ (and chloride) accumulated in the vacuole to drive water into the cells (*2*). This Na^+/H^+ antiport transports Na^+ into the vacuole by using the electrochemical gradient of protons generated by the vacuolar H^+-translocating enzymes, H^+–adenosine triphosphatase (ATPase) and H^+–inorganic pyrophosphatase (PP_iase) (*3, 4*). Vacuolar Na^+/H^+ antiport activity was shown first in tonoplast vesicles from red beet storage tissue (*5*) and later in various halophytic and salt-tolerant glycophytic species (*6, 7*). Chloride transport into the vacuole is mediated by anion channels (*8*). In *Arabidopsis*, a vacuolar chloride channel, AtCLCd, similar to the yeast Gef1, has been cloned (*9*). The analysis of genes involved in cation detoxification in yeast led to the identification of a novel Na^+/H^+ antiport (Nhx1). Nhx1 was localized to a prevacuolar compartment and showed a high degree of amino acid sequence similarity to Na^+/H^+ antiports from *Caenorhabditis elegans* and humans (NHE6, mitochondrial) (*10*). Recently, the *Arabidopsis thaliana* genome-sequencing project has allowed for the identification of a plant gene (*AtNHX1*) homologous to the *Saccharomyces cerevisiae Nhx1* gene product (*11–13*). Both Nhx1 and Gef1 are localized to the yeast prevacuolar compartment, suggesting a role for this compartment in salt tolerance. Overexpression of *AtNHX1* suppresses some of the salt-sensitive phenotypes of the Δ*nhx1* yeast strain (*13*), suggesting that the plant and the yeast gene products might be functionally similar.

AtNHX1 transcripts are found in root, shoot, leaf, and flower tissues (*11*). To determine the subcellular localization of AtNHX1, we immunoblotted membrane fractions (*14*) isolated from wild-type plants and plants overexpressing AtNHX1 (*15*) with antibodies raised against the COOH-terminus of AtNHX1 (Fig. 1). A protein of an apparent molecular mass of 47 kD was detected mainly in the tonoplast- and Golgi/endoplasmic reticulum (ER)–enriched fractions, and was more abundant in the transgenic plants. No noticeable cross-reactivity

Department of Botany, University of Toronto, 25 Willcocks Street, Toronto, Ontario M5S 3B2, Canada.

*These authors contributed equally to this work.
†To whom correspondence should be addressed. E-mail: blumwald@botany.utoronto.ca

Downloaded from www.sciencemag.org on April 28, 2009

with these antibodies was observed in plasma membrane– and mitochondria-enriched fractions, which suggests that the plant NHX1 does not share the same subcellular localization as that determined for NHE6 (*16*). It remains unclear whether the immunoreactive protein observed in the Golgi/ER-enriched fractions represents contamination of this fraction with tonoplast proteins (*5*) or presence of the target protein in prevacuolar compartments. Nonetheless, immunoblots of purified leaf vacuoles (*17*) from transformed plants showed more *AtNHX1* gene product than those from wild-type plants (Fig. 1B). The apparent molecular mass (47 kD) of AtNHX1 is somewhat lower than that predicted by the amino acid sequence of the *AtNHX1* open reading frame (58 kD) and may reflect anomalous migration in the SDS–polyacrylamide gel electrophoresis (SDS-PAGE) gel (*18*) or specific cleavage (or degradation).

In order to assess whether AtNHX1 provides a Na^+/H^+ exchange function, Na^+-dependent H^+ movements (*19*) were measured in vacuoles isolated from the leaves of wild-type plants and plants overexpressing AtNHX1 (Fig. 2). The Na^+/H^+ exchange rates were very low in vacuoles from wild-type plants (Fig. 2A, trace 1). In contrast, Na^+/H^+ exchange rates were much higher in vacuoles from the transgenic plants (Fig. 2A, trace 2). The Na^+/H^+ antiport activity was not affected by the presence of 30 mM K^+ ions in the assay medium (*20*), indicating selectivity for Na^+. Electroneutral Na^+/H^+ exchange is suggested by the similar rates of Na^+-dependent H^+ movements obtained when the membrane potential was clamped by the addition of 1 μM valinomicyn and 2 mM K^+ to the assay medium (*20*). The Na^+ dependence of the H^+ flux is evidence of a Na^+/H^+ antiport mechanism. The Na^+/H^+ exchange displayed Michaelis-Menten kinetics with respect to extravacuolar Na^+ concentrations (Fig. 2B). Similar apparent K_m values of the exchanger for Na^+ were obtained with two independent transgenic lines, K_m = 7 mM (Fig. 2C) and 6.1 mM (*20*). These values are of the same order of magnitude as those reported for other plant species (*7*). The relative increase in protein abundance (Fig. 1B) is less than the increase in Na^+/H^+ antiport activity measured in vacuoles from transgenic plants (Fig. 2, A and B). These observations suggest that in wild-type plants under normal growth conditions, AtNHX1 function may be repressed. Overexpression of AtNHX1 may overcome this endogenous repression mechanism.

Salt tolerance was tested in wild-type and transgenic plants overexpressing *AtNHX1* (Fig. 3). Wild-type plants displayed progressive chlorosis, reduced leaf size, and a general growth inhibition when watered with a NaCl-containing solution. These inhibitory effects increased progressively with the increasing NaCl concentration in the watering solution. The transgenic plants were unaffected by up to 200 mM NaCl (Fig. 3, lower panel) and plant development was not compromised, as the transgenic plants bolted and set seed in all salt treatments. However, transgenic plants grown at 300 mM NaCl displayed a reduction in leaf size and chlorosis (*20*). The three independent transgenic lines showed a similar increase of *AtNHX1* transcript levels (Fig. 3, inset) and similar salt tolerance (*20*). The Na^+ content of both wild-type and transgenic plants increased with exposure to high NaCl (Fig. 4). The higher Na^+ content of the transgenic plants growing in 200 mM NaCl, together with the sustained growth (Fig. 3) and

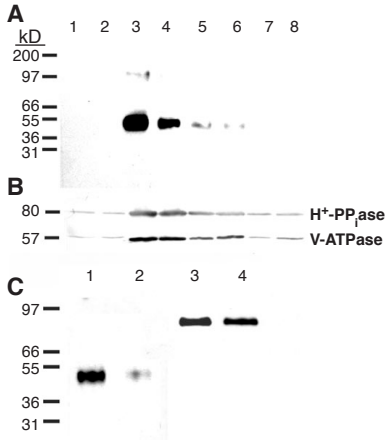

Fig. 1. Subcellular localization of AtNHX1. (**A**) Membrane fractions were isolated from shoots of 5-week-old seedlings (*14*). Protein (5 μg) was separated on a 10% SDS-PAGE and electroblotted. Polyclonal antibodies, raised against the COOH-terminal portion of AtNHX1 (*21*), were used for the immunoblot, which was developed using chemiluminescence. The lane numbers correspond as follows: Lanes 1 and 2, mitochondria; lanes 3 and 4, tonoplast-enriched fraction; lanes 5 and 6, Golgi/ER-enriched fraction; lanes 7 and 8, plasma membrane–enriched fraction. Odd-numbered lanes correspond to membrane fractions isolated from plants overexpressing AtNHX1, while even-numbered lanes correspond to fractions isolated from wild-type plants. (**B**) Enrichment of the fractions with tonoplast membranes was assessed with antibodies raised against the vacuolar H^+-PP_iase and the vacuolar V-ATPase. (**C**) Purified vacuoles (*17*) were pelleted and solubilized in SDS-PAGE sample buffer. Protein (3 μg) was resolved on 10% SDS-PAGE and immunoblotted. Lanes 1 and 3 correspond to vacuolar membranes isolated from plants overexpressing AtNHX1, while lanes 2 and 4 correspond to vacuolar membranes isolated from wild-type plants. Lanes 1 and 2 show immunoreaction with antibodies raised against AtNHX1. Lanes 3 and 4 show immunoreaction to antibodies raised against the vacuolar H^+-PP_iase. Relative molecular masses are indicated on the left.

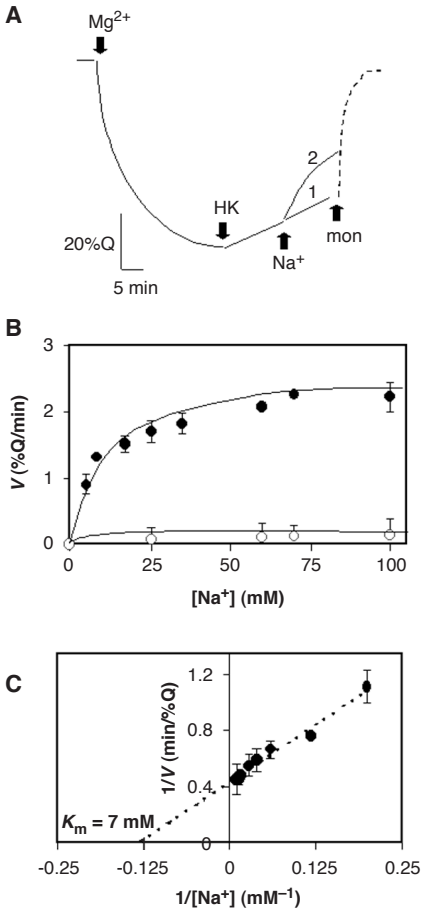

Fig. 2. The Na^+/H^+ exchange activity in leaf vacuoles from wild-type plants and plants overexpressing AtNHX1. (**A**) The fluorescence quenching of acridine orange was used to monitor the dissipation of inside-acid pH gradients across the vacuoles. Vacuoles (5×10^4) were added to 0.8 ml buffer containing 0.3 M mannitol, 2 mM dithiothreitol, 5 mM Tris/MES buffer (pH 8.0), 5 mM glucose, 30 mM tetramethylammoniuim chloride, 1.5 mM Tris-ATP, and 5 μM acridine orange. Proton translocation was initiated with the addition of 3 mM Mg^{2+} and the change of fluorescence with time was monitored as described (*19*). When a steady-state pH gradient (acidic inside) was formed, the ATP-dependent H^+ transport activity was stopped by the addition of hexokinase (HK) (*19*). After a constant rate of fluorescence recovery was obtained, aliquots of 5 M NaCl (Na^+) were added, and the changes in fluorescence recovery were determined (*19*). The addition of monensin (mon), an artificial Na^+/H^+ antiport, abolished the pH gradient and the fluorescence was fully recovered. The figure shows a typical recording; gaps in the lines indicate the addition of reagents. Curves labeled 1 and 2 indicate vacuoles from wild-type plants and from plants overexpressing AtNHX1, respectively. (**B**) Kinetics of Na^+/H^+ exchange in vacuoles from wild-type plants (○) and plants overexpressing AtNHX1 (●). Each point represents the mean ± SD (n = 3). (**C**) Double reciprocal plot of the Na^+-dependent recovery of acridine orange fluorescence quenching. Each point represents the mean ± SD (n = 3). The apparent K_m was calculated by the intersection of the fitted line with the abscissa. % Q, percentage of fluorescence quenching.

Downloaded from www.sciencemag.org on April 28, 2009

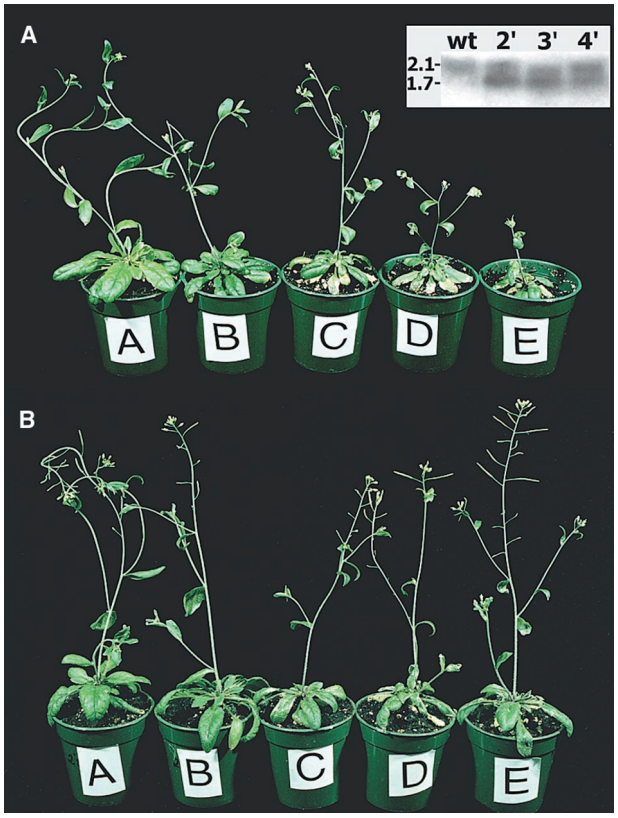

Fig. 3. Salt treatment of wild-type plants and plants overexpressing AtNHX1. Transgenic T3 plants from the lines overexpressing AtNHX1 were used in assessing salt tolerance. Twenty wild-type plants and 20 of each of the three lines of transformed plants overexpressing AtNHX1 were grown on a short-day cycle (8 hours light, 16 hours dark). Each set of 20 plants was divided into five groups (labeled A through E) of four plants each. We applied 25 ml of a diluted nutrient solution (1/8 MS salts) every other day over the 16-day watering treatment. The control group received no NaCl supplementation. The remaining groups were watered with nutrient solution supplemented with NaCl. The concentrations of NaCl supplementation were increased stepwise by 50 mM every 4 days for each group, to the indicated maximum: (A) control, (B) 50 mM NaCl, (C) 100 mM NaCl, (D) 150 mM NaCl, and (E) 200 mM NaCl. The salt-tolerance phenotype was observed in three independent transgenic lines tested. The transgenic line shown (2′) is representative of the three tested lines as are the plants from each treatment group. (**A**) (upper panel) Wild-type plants. (**B**) (lower panel) Plants overexpressing AtNHX1. (**Inset**) Northern blot of RNA isolated from leaves of wild-type (wt) and three independent lines (2′; 3′; 4′) of transgenic plants grown in the absence of NaCl. RNA was probed with *AtNHX1* cDNA. Equal amounts of total RNA were present in each sample (30 μg). In all plants, the endogenous 2.1 kilobase (kb) transcript was detected. An additional transcript of ~1.7 kb that corresponds to the predicted open reading frame of AtNHX1 can be seen only in the transgenic plants. Apparent molecular size (kb) of the transcripts is indicated to the left.

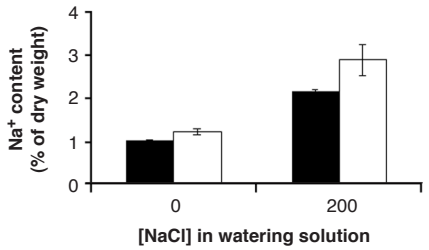

Fig. 4. The Na^+ content in wild-type (black bars) and transgenic plants (white bars) grown in the absence or presence of 200 mM NaCl. The aboveground parts of the plants were harvested at the end of the salt treatment. Dry weight was measured after 24 hours at 70°C, and Na^+ content was determined by atomic absorption spectrophotometry. Values are the mean ± SD (n = 4).

the increased vacuolar antiport activity (Fig. 2), is consistent with increased vacuolar compartmentation of Na^+ in the transgenic plants. We did not detect an increase in *AtNHX1* transcript levels in response to NaCl (50 to 250 mM) (*13*) or upon the application of exogenous ABA (*20*). We have analyzed RNA from young seedlings and mature plants, and from the roots, shoots, and leaves of NaCl-stressed plants at different time points (6 to 36 hours) grown in petri dishes or in soil. No increase in the *AtNHX1* protein product was detected either by immunoblotting or by vacuolar Na^+/H^+ activity assays in response to NaCl-stress (*20*). These results would suggest that the induction of AtNHX1 protein synthesis or vacuolar Na^+/H^+ antiport activity in response to NaCl-stress in *Arabidopsis* wild-type plants requires conditions which are currently unknown. Since *Arabidopsis* is a glycophytic plant with a sensitivity to salt similar to most crop plants, our findings suggest the feasibility of genetic engineering crop plants with improved salt tolerance.

References and Notes

1. R. G. Wyn Jones, in *Physiological Processes Limiting Plant Productivity*, C. B. Johnson, Ed. (Butterworths, London, 1981), pp. 271–292.
2. E. Glenn, J. J. Brown, E. Blumwald, *Crit. Rev. Plant Sci.* **18**, 227 (1999).
3. E. Blumwald, *Physiol. Plant.* **69**, 731 (1987).
4. P. A. Rea and D. Sanders, *ibid.* **71**, 131 (1987).
5. E. Blumwald and R. J. Poole, *Plant Physiol.* **78**, 163 (1985).
6. B. J. Barkla and O. Pantoja, *Annu. Rev. Plant Physiol. Plant Mol. Biol.* **47**, 159 (1996).
7. E. Blumwald and A. Gelli, *Adv. Bot. Res.* **25**, 401 (1997).
8. P. J. Plant, A. Gelli, E. Blumwald, *J. Membr. Biol.* **140**, 1 (1994).
9. M. Hechenberger *et al.*, *J. Biol. Chem.* **271**, 33632 (1996).
10. R. Nass, K. W. Cunningham, R. Rao, *ibid.* **272**, 26145 (1997).
11. M. P. Apse, G. S. Aharon, W. A. Snedden, E. Blumwald, *Proceedings of the 11th International Workshop on Plant Membrane Biology*, Cambridge, UK, 9 to 14 August 1998 (Society for Experimental Biology, London, 1998), p. 84.
12. C. P. Darley, D. van Wuyt Swinkel, K. Van der Woude, P. Mager, B. de Boer, *ibid.*, p. 8.
13. R. A. Gaxiola *et al.*, *Proc. Natl. Acad. Sci. U.S.A.* **96**, 1480 (1999). GeneBank accession number AF106324.
14. Membrane proteins were purified from 5-week-old *Arabidopsis thaliana* plants using the method described (*5*) with the following modifications. Tonoplast-, Golgi/ER-, and plasma membrane–enriched fractions were obtained from the 0%/20%, 20%/30%, and 30%/40% interfaces, respectively. Chymostatin, leupeptin, aprotinin, and pepstatin (each to a 10 μM final concentration) were added to the resuspension buffer.
15. The open reading frame sequence obtained by our lab is identical to that recently described by Gaxiola *et al.* (*13*). The *AtNHX1* putative open reading frame was amplified by polymerase chain reaction (PCR) from the cDNA template and cloned into the Sal I/Sma I sites of pBISN1 [S. B. Narasimhulu, X. Deng, R. Sarria, S. B. Gelvin, *Plant Cell* **8**, 873 (1996)] in a sense orientation using the following primers: *Se-ATX1*-5′-CGCGTCGACATGTTGGATTCTCTAGTGTCG-3′ and *AtXCT2*-5′-CGGAATTCTCAAAGCTTTCTTCCACG-3′. The resulting vector contained *AtNHX1* under the control of the supermas promoter. *Agrobacterium*-mediated transformation was performed using flowering plants with primary bolts reaching 15 cm. Plants were dunked into a bacterial solution, for 5 min, containing 0.5× Murashige and Skoog (MS) salts; 0.5 g/liter MES; 5% sucrose and 0.03% Silwet. The same procedure was repeated 12 days later. Transgenic plants were selected by plating the seeds on 0.5× MS agar plates containing 25 mg/liter kanamycin. Plants were carried for two more generations in order to identify plants homozygous for the transgene.
16. M. Numata, K. Petrecca, N. Lake, J. Orlowski, *J. Biol. Chem.* **273**, 6951 (1998).
17. Vacuoles were isolated by osmotic lysis of leaf protoplasts and floated on top of a 2% Ficoll cushion as described (*19*).
18. R. Ros, C. Montesinos, A. Rimon, E. Padan, R. Serrano, *J. Bacteriol.* **180**, 3131 (1998).
19. E. Blumwald, E. J. Cragoe Jr., R. J. Poole, *Plant Physiol.* **85**, 30 (1987).
20. M. P. Apse, G. S. Aharon, E. Blumwald, data not shown.
21. Antibodies were raised in rabbits against a glutathione *S*-transferase (GST)–fusion protein of the COOH-terminal region of AtNHX1. These fusion proteins were produced in *Escherichia coli* (strain BL21pLysS) that had been transformed with the pGEX2TK, into which we had subcloned the region encoding the final 95 amino acids of AtNHX1. The Eco RI–Bam HI fragment of the PCR product amplified from the cDNA template using the PCR primers, forward-5′-CGGGATCCCCGCACCAGAACGCCACC-3′ and reverse-AtXCT2 (*15*), was ligated into the same sites on the pGEX2TK vector. Induction and purification of the recombinant GST-fusion was as per manufacturers instructions (Pharmacia). Antibodies were purified by first passing the antiserum over an immobilized GST column (Pierce), and then by affinity blot purification [E. Harlow and D. Lane, *Antibodies: A Laboratory Manual* (Cold Spring Harbor Laboratory Press, New York, 1988), p. 498].

22. We thank P. A. Rea for the antibodies raised against the H^+-PP_iase and M. Manolson for antibodies raised against the V-ATPase. Supported by an operating grant from the Natural Sciences and Engineering Research Council of Canada to E.B.

28 April 1999; accepted 7 July 1999

Downloaded from www.sciencemag.org on April 28, 2009